Tuning of Carbon Microspheres and Graphene Structures with Hetero Atoms for Organic Dye Degradation and Heavy Metal Remediation - Influence of Fructose as a Precursor

S. Sudhaparimala† and R. Usha

Department of Chemistry, Ethiraj College for Women, University of Madras, Chennai-600008, Tamil Nadu, India
†Corresponding author: S. Sudhaparimala; sudha92@gmail.com

ABSTRACT

In today's context, there is a tremendous potential for the design of smart nanomaterials of carbon origin for multi-dimensional applications. The role-play of precursor is significant in the design of nanometric carbon materials apart from other experimental parameters. Correlation of the synthetic methodology, the microstructure of the product helps to tune and widen the applications aspect. The present study aimed to tune the simple ketose (reducing monosaccharide) of fructose to functionalize (with O, N, and S atoms) carbon layers, microspheres of carbon, to optimize the experimental conditions, and to establish the mechanism involved in the process. The study further explored the catalytic ability of the carbon samples in the degradation of thiazine and xanthene-based textile dyes and the sensing of heavy metal ions of chromium and copper. A simple hydrothermal process, fructose as a precursor, alkaline pH, and appropriate calcination temperature provided micro and nanostructures of carbon viz. carbon microspheres (CMs), graphene oxide (GO), sulfur doped graphene oxide (S-GO), and nitrogen-doped reduced graphene oxide (N-rGO). In this study a simple mechanism for the conversion process is suggested. Further, the results of the preliminary screening study on the catalytic ability of the sulfur and nitrogen-doped graphene samples in the presence of UV and Visible light upon the degradation of methylene blue (MB), methyl orange (MO), Rhodamine-B (Rh-B) dyes were satisfactory. The adsorbent and the ion exchange capacity of the carbon microspheres were found to be excellent. The results of the study will contribute positively to the treatment and management of industrial wastewater.

INTRODUCTION

In recent years, among the carbon-based nanomaterials, two-dimensional graphene has received significant attention due to its unique optical, electronic, mechanical, and thermal properties used in many fields such as catalysis, nanoelectronics, sensors, capacitors, and nanocomposites. There are only a few recent research reports available on the use of synthetic carbohydrates (aldose and ketose) as a precursor for the synthesis of carbon-based nanomaterials, graphene in particular. Sunil et al. (2020) reported the synthesis of reduced graphene oxide from glucose as a precursor by the hydrothermal method and suggested a reaction mechanism. Mingfei et al. (2020) reported that the green precursor of fructose was used for the synthesis of carbon quantum dots by the hydrothermal method. There are no reports available to date on synthetic fructose as a precursor for the synthesis of 2D carbon nanomaterial (graphene-based nanomaterials) by hydrothermal method. Sudhaparimala and Usha (2021) reported a facile synthetic approach to the functionalization of graphene with the atoms of Oxygen and sulfur from the reducing monosaccharide of glucose as a precursor for the catalytic removal of Chlorophenols and textile dyes.

There is also a broader scope for reducing monosaccharides of fructose as the resource for the design of graphene-based materials. In this context, there is a need to understand the first principles in building graphene structures with non-metal atoms of O, S, and N for tailoring their applications. Such a study will enhance the scope of biomass conversion to bio graphene-based materials since the glucosidal or fructosidal monosaccharides with active functional groups are the basic units of biomass.

Taking into consideration the above factors, the present research study provides a simple approach for the building of graphene layers with non-metal atoms of O, S, and N doped and spherical carbon microspheres from the precursor of fructose. Based on the analytical scrutiny of the microstructures a mechanistic pathway has been suggested. A correlative study between these structural aspects and their application as an adsorbent and photocatalyst in the degradation of toxic dyes and the ability to sense the presence of heavy metal ions has been successfully carried out.

Wastewater from the textile industry contains dyes mixed with various contaminants at a variety of ranges while paper and textile industries contribute dyestuffs of thiazine, azo and xanthene origin and their complete degradation is challenging globally. Degradation of simple representative examples of such dyes being Methylene blue, Methyl orange, and Rhodamine-B have been reported respectively (Bharatia et al. 2017).

Among all the pollutants, heavy metals have also received paramount attention from environmental chemists due to their toxic nature. Metals such as arsenic (As), lead (Pb), cadmium (Cd), nickel (Ni), mercury (Hg), chromium (Cr), cobalt (Co), zinc (Zn), and selenium (Se) become toxic when they are not metabolized by the body and accumulate in the soft tissues. They may enter the human body through food, water, air, or absorption through the skin when they come in contact with humans in agriculture, manufacturing, pharmaceutical, industrial or residential settings (Van Ael et al. 2012) Fabrication of the 2D carbon materials for sensing and ion exchange medium will open up another dimension to their applications. Existing reports on such applications are limited.

Considering these factors, there is a need to develop a new, efficient economic, and green catalyst. A new approach to the synthesis of functionalized graphene from a much-unexplored precursor of fructose and their ability to function as efficient adsorption and photocatalyst in the dye degradation is considered. In this current study, the simple monosaccharide of fructose (ketose) was used as a precursor for the synthesis of 2D carbon-based nanomaterials (CBNs) doped with non-metal atoms of O, N, S, and carbon microspheres by a simple hydrothermal method. The study was also undertaken to suggest a reaction pathway, screen them for the degradation of organic dyes, sensing of heavy metal ions by simple experimental methods. The results of the study will enhance the understanding of biomass conversion to smart materials and tailoring them for industrial wastewater management.

MATERIALS AND METHODS

Materials

Chemicals used for the synthesis of carbon microspheres and graphene-based nanomaterials (GBNs) are fructose (Merck chemicals), sulfuric acid (H_2SO_4), sodium hydroxide (NaOH) (Nice chemicals), glacial acetic acid (Nice chemicals), 99.9% ethanol (Analytical CS reagent), ammonia (NH_3), methylene blue (MB) stain (Merck chemicals), methyl orange (Nice Chemicals), Rhodamine Black (Merck Chemicals), calcium carbonate (Spectrum), magnesium sulfate (Nice chemicals),

copper sulfate (Nice chemicals), zinc sulfate (Nice chemicals), buffer solution (pH=10) potassium dichromate (Nice chemicals), ethylene diamine tetraacetic acid (EDTA) (Nice chemicals), Eriochrome black-T (EBT) (Nice chemicals).

Method of Synthesis

Preparation of functionalized carbon microspheres (CMs) and functionalized graphene-based nanomaterials (GO, S-GO, N-rGO) by hydrothermal method

The experimental conditions were optimized for the synthesis of carbon-based nanomaterials using fructose by changing the reaction parameters like pH and temperature by hydrothermal method. Two samples were collected at the end of the process based on the decomposition temperature of the fructose at 180°C (GO) and 220°C (CMs) respectively at pH at 9 (adjusted by adding sodium hydroxide) for 5 h. The black solid sample (carbon microspheres (CMs) was obtained at 220°C (Sudhaparimala & Usha 2020).

For doping with sulfur, the graphene oxide (GO) (brown gel) sample obtained from hydrothermal treatment was treated with sulfuric acid in the ratio of 1:5 and heated at 80°C. The black solid residue obtained upon doping (GO-180°C) was further dried at room temperature. For the introduction of nitrogen, about 0.5 M fructose solution was hydrothermally heated after adding liquid ammonia in the ratio of 1:10, at 220°C for 5 h at pH=9 resulting in a resultant brown solid sample.

All the four product samples namely brown gel graphene oxide (GO) sample and brownish-black solid samples of sulfur-doped graphene oxide (S-GO), nitrogen-doped reduced graphene oxide (N-rGO) and carbon microspheres (CMs) were treated with ethanol for the removal of organic impurity. The samples were then refrigerated and stored for further characterization.

Material Characterization

The functional groups, bonding characteristics, and structural defects in the as-synthesized functionalized GBNs (GO, S-GO, and N-rGO) and carbon microspheres (CMs) were analyzed using the FT-IR (IR Affinity-1, Shimadzu) and Micro-Raman spectrometer (Bruker, RFS). The Avance III 500 NMR spectrometer was used for structural analysis. The microstructural analysis was carried out using powder X-ray diffractogram (PXRD) using a Cu-K radiation (PAN analytical model Xpert pro), surface morphology using a Field Emission Scanning Electron Microscopic (SEM) (Fei Quanta), and transmission electron microscopic (TEM) (Joel) image. The surface elemental composition and chemical state of the elements were identified using X-ray photoelectron

spectroscopy (XPS) (Ulvac-Phi, Inc.; Model: PHI5000 Version Probe III). The decolorization efficiency of the synthesized samples upon organic dyes under dark and light (UV and Sunlight) were screened with respect to time and also screened for the sensing capability of metal ions using colorimetry (Photometer μM).

Screening the photocatalytic efficiency of the carbon microspheres, oxygen and sulfur, nitrogen-doped graphene (GO, S-GO And N-rGO) as a catalyst on the decolorization of textile dyes

The as-synthesized samples of carbon microspheres and functionalized GBNs (S-GO, N-rGO) were screened individually for their catalytic activity in the discoloration of methylene blue (MB), methyl orange (MO), Rhodamine-Black (Rh-B) solution (2 ppm). The catalyst and the dye solution were taken in the ratio of 2mg/10mL (w/v) and the reaction mixtures were incubated in dark, UV, and sunlight medium at a pH of 3. The discoloration efficiency was measured in terms of optical density units for every half an hour for a total duration of two hours.

Detection of toxic metal ions (copper and chromium) by colorimetric method

The sensing efficiency of the samples for the metal ions of copper (Cu^{2+}) and chromium (Cr^{6+}) ion was screened by colorimetric method using different concentrations of copper sulfate (300 mM, 100 mM, and 50 mM) and potassium dichromate (50 mM, 10 mM, 0.1 mM, 0.01 mM) solution respectively. The optical density values were measured and compared with and without using as-synthesized samples (CMs, S-GO, N-rGO) as a catalyst in the concentration of 100 ppm (w/v).

Estimation of calcium and magnesium ion using assynthesized samples as a catalyst

The ions of Calcium and Magnesium were estimated by the usual EDTA titration using EBT indicator with and without the presence of synthesized samples (CMs, S-GO, N-rGO) at different concentrations (100 ppm, 200 ppm, 300 ppm, 400 ppm, 500 ppm). The role-play of the CBNs was studied using FT-IR spectra of the recovered samples after the estimation of metal ions.

RESULTS AND DISCUSSION

The basic structural aspects, microstructural and morphology of the as-synthesized samples of graphene oxide at 180°C (GO), carbon microspheres at 220°C (CMs), sulfur-doped graphene oxide at 180°C (S-GO), and nitrogen-doped reduced graphene oxide at 220°C (N-rGO) were analyzed.

FT-IR spectra of the precursor (fructose), assynthesized carbon microspheres and functionalized GBNs (GO, S-GO and N-rGO)

The functional groups corresponding to C-O, C=O, C=C, O-H, C-H in as-synthesized samples were identified and represented in Fig. 1(a). The intensity of the bands corresponding to C-O, C=O, O-H has decreased with respect to the precursor which signifies a decrease in oxygen functionality in all the as-synthesized samples (Mohammed 2014, Hassan et al. 2014, Sudhaparimala & Usha 2020). The band at 796cm^{-1} due to C=S group (Rao et al. 1963) and 2225cm^{-1}, 1395cm^{-1} due to stretching vibrations of graphitic carbon nitride and C=N functional groups were identified in S-GO and N-rGO respectively. In N-rGO, the band corresponding to C=C has increased when compared with S-GO indicating the decrease in the number of sp^2 carbon upon doping with sulfur. (Vasilios et al. 2015)

Micro-Raman spectra of as-synthesized Carbon Microspheres and functionalized GBNs (S-GO and N-rGO)

Micro-Raman spectrum is used as a characterization tool for analyzing the nature, amount, and types of structural defects present in graphene-based nanomaterials. In Fig. 1(b) the G-band of the micro-Raman spectra represents allowed high-frequency E_{2g} phonon of sp^2 carbon and D-band represents A_{1g} phonons around the Brillouin zone corner K and is activated by an intravalley double resonant process of sp^3 carbon, the 2D band represents overtone of D band, D' band coming from the intravalley double resonant process of E_{2g} phonon (Mark et al. 2011).

The I_D/I_G ratio indicates that the amount of defects has increased on doping with sulfur and decreased on doping with nitrogen. It may be due to the higher electronegativity of nitrogen compared to a sulfur atom which was well correlated with FT-IR analysis also. From the I_{2D}/I_G ratio, the numbers of layers in as-synthesized graphene nanomaterial were analyzed which increased functionalization with sulfur. It further indicates the decrease in the number of layers and the presence of sulfur-based functional groups at the edges of the plane of graphene (Erick et al. 2020, Isaac et al. 2013, Zhangting & Zhenhua 2017). The ratios of I_D/I_G, $I_D/I_{D'}$ and I_{2D}/I_G of synthesized carbon microspheres and functionalized GBNs are presented in Table 1.

From the results, the $I_D/I_{D'}$ ratio was found to be less than 3.5(< 3.5) for all the GBNs. The samples have a one-dimensional defects as observed in the grain boundaries of the synthesized graphene nanomaterials. The average defect distance has increased on functionalization which confirmed

Table 1: Comparison of the Intensity ratio of I_D/I_G, I_{2D}/I_G, and $I_D/I_{D'}$ of the as-synthesized samples.

Name of the sample	I_D/I_G ratio	I_{2D}/I_G ratio	$I_D/I_{D'}$ ratio	Average defect distance (L_D in nm)
CMs	0.3424	0.9498	0.6903	23.6952
GO	1.2714	0.9614	2.9820	12.2965
S-GO	0.9796	0.9796	1.3373	13.7713
N-rGO	0.4166	0.6736	0.5814	21.4800

the defects in the edges of the graphene plane and not in the basal plane (Isaac et al. 2013, Zhangting & Zhenhua 2017).

Carbon-13 Nuclear Magnetic Resonance (C-13 NMR) spectrum of graphene oxide

The C-13 NMR spectrum of the as-synthesized of graphene oxide is presented in Fig. 1(c). The NMR of the gel obtained at 180°C showed chemical shift value due to cyclodextrin with more number of layers and the results well correlated with the report (Anton et al. 2019).

The presence of sp^2 carbon was indicated by the peak in the range of 100-150 ppm The Oxygen functionality in the graphitic structure was identified in the range of 60-90ppm with 37 NMR peaks due to GO (Tapas et al. 2016, Guangxu et al. 2018). From the NMR result, it is established that the gel form of oxygen functionalized graphene obtained at 180°C is an intermediate in the formation of the final product of solid graphene oxide. The result correlated well with FT-IR and micro-Raman analysis. The confirmation from the NMR study is the first report of its kind in the synthesis of GO samples from fructose as a precursor by the hydrothermal method. It aids in the suggestion of a mechanistic pathway for the functionalization of graphene layers using non reducing monosaccharides.

Powder X-ray Diffraction (PXRD) spectra of synthesized GBNs and Carbon Microspheres Samples

The PXRD spectrum of the as-synthesized samples was given in Fig. 1(d). It can be seen that the 2θ values increased upon functionalization with sulfur or nitrogen on graphene. The d-spacing value has decreased on doping with sulfur and nitrogen which indicates that the functional groups are present at the edges and not in the basal plane of graphene. As the size of the doping element increased, the d–spacing value decreased thus increasing structural defect which was well correlated with the Micro-Raman analysis of graphene-based nanomaterial (Guangxu et al. 2018, Agata et al. 2017). The broadness of the peak has increased in the functionalized carbon nanomaterials (S-GO and N-rGO) than carbon microspheres (Mohammed 2014, Hassan et al. 2014, Erick et al. 2020). The 2θ values, d-spacing value, and miller indices of the as-synthesized samples are presented in Table 2.

High-Resolution Scanning Electron Microscopic (HR-TEM) and Field Emission Scanning Electron Microscopic (FE-SEM) images of the as-synthesized samples

The surface morphology of the as-synthesized samples as presented in Fig. 2 indicated a perfect, uniform spherical well-dispersed morphology of the carbon microspheres (CMs) (Fig. 2b) which correlates with the report (Shunji-an et al. 2015, Sanja et al. 2015). The layer structures of graphene oxide were observed in Fig. 2a and correlate with a report (Tapas et al. 2016). The layer structure with spherical aggregates were observed in S-GO (Fig.2c) (Qinghong et al. 2018, Sudhaparimala & Usha 2020). In the case of N-rGO, layer structure with spherical dots (Fig.2d) were observed indicating more surface defects with less microstructural defects as indicated by micro raman analysis (Fig.1(b)) (Guangxu et al. 2018).

Wide scan X-ray Photoelectron spectroscopic (XPS) images of Carbon Microspheres, Sulfur-doped graphene Oxide, and Nitrogen-doped reduced graphene Oxide

Wide scan X-ray photoelectron spectroscopic images of carbon microspheres (CMs), sulfur-doped graphene oxide (S-GO), and nitrogen-doped reduced graphene oxide (N- rGO) are given in Fig. 3. The binding energy value corresponding to C (1s) was identified due to alkane (284.6 eV), alkene (285.9 eV) was hydroxyl (285.6 eV), epoxy (286.3eV), carbonyl (287.3eV), Carboxyl (289.1eV) indicating the presence of functional groups on the surface of assynthesized samples. The additional binding energy peak corresponding to C-S was identified at 285.4eV in S-GO and C-N peak was identified at 287.7eV in N-rGO confirming the doping of the heteroatoms of sulfur, and nitrogen respectively and it correlates with the reports (Agata et al. 2017, Qinghong et al. 2018, Ho et al. 2011).

Table 2: Comparison of d-spacing, 2θ value, and miller indices of the as-synthesized samples.

Name of the sample	2θ	d-spacing	Miller indices
CMs	19.6567°	0.3963	001
S-GO	20.3087°	0.3932	001
N-rGO	20.1325°	0.3916	001

The defect on the surface of the as-synthesized samples was confirmed using the intensity ratio of sp^3/sp^2 carbon using C (1s) XPS spectrum (Agata et al. 2017). It can be seen that the one-dimensional grain boundaries defect in graphene structure increased on doping upon more with sulfur than nitrogen due to the electronegativity difference between the atoms which is well correlated with Micro-Raman analysis. The presence of carboxyl and carbonyl functional groups was profound in S-GO while hydroxyl, epoxy groups are prominent in N-rGO as confirmed by broad scan X-ray photoelectron spectroscopic image of O(1s). The layer with more spherical aggregates was introduced upon functionalization with sulfur than nitrogen. The intensity ratio of sp^3/sp^2 carbon from XPS was compared with the I_D/I_G ratio obtained from Micro-Raman analysis and carbon to oxygen ratio on the surface of the synthesized samples from XPS and EDX analysis as presented in Table 3.

The carboxy and carbonyl functional groups were present at higher concentrations on the surface of CMs and S-GO. The hydroxyl and epoxy groups were found to be high in the case of N-rGO, which indicates that the functional groups present at the edges are not in the basal plane which correlates with PXRD reports. The C/O ratio was comparatively less on doping with sulfur than nitrogen which correlates well with EDX analysis it is clear that the increased C/O ratio of nitrogen-doped reduced graphene oxide indicates the more reduction of oxygen functionality by the introduction of nitrogen than sulfur due to the greater size and electronegativity of the elemental nitrogen. (Agata et al. 2017)
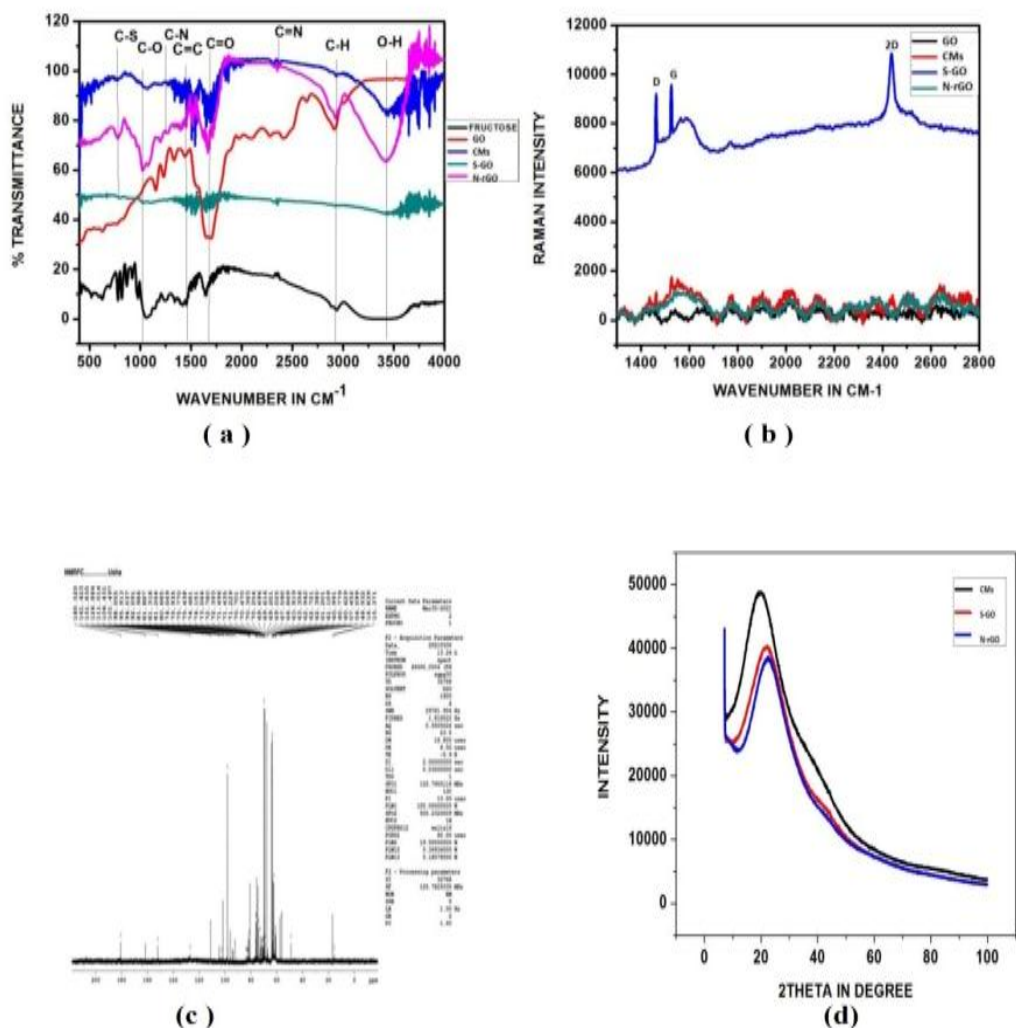

Fig. 1: (a) FT-IR- spectrum of fructose, CMs, GO, S-GO, N-rGO, (b) micro-Raman spectrum of CMs, GO, S-GO, N-rGO, (c) carbon-13 NMR spectrum of graphene oxide, (d) PXRD spectrum of CMs, S-GO, N-rGO.

Table 3: Comparison of carbon to oxygen ratio from EDX and XPS analysis and compared the intensity ratio of sp^3/sp^2 carbon from XPS analysis and I_D/I_G ratio from Micro-Raman analysis of the as-synthesized samples.

Name of the sample	Name of the element	Percentage of elements from wide scan spectrum of XPS analysis	Percentage of elements from EDX analysis	C/O ratio from wide scan spectra of XPS analysis	C/O ratio from EDX analysis	sp^3/sp^2 ratio from XPS analysis	I_D/I_G ratio from micro-Raman analysis
CMs	Carbon	68.83	79.16	2.1922	3.7985	1.5113	1.2714
	Oxygen	31.17	20.84				
S-GO	Carbon	49.88	59.55	1.2121	1.7351		
	Oxygen	41.15	34.32			1.6484	0.9796
	Sulfur	8.9637	6.13				
N-rGO	Carbon	47.77	78.37	1.2143	3.9521		
	Oxygen	39.34	19.83			1.5015	0.4166
	Nitrogen	12.88	1.8				

The above characterization reports confirm the microstructure of graphene oxide (GO), sulfur-doped graphene oxide (S-GO), nitrogen-doped reduced graphene oxide (N-rGO), and carbon microspheres (CMs) were synthesized by hydrothermal method. Based on the properties, the as-synthesized solid samples of CMs, S-GO, N-rGO were screened as adsorption and photocatalyst for the decoloration of dyes and used as adsorption catalysts for the detection of heavy metal ions.

From the above results, the following reaction mechanism is suggested for the synthesis of graphene oxide, sulfur-doped graphene oxide, and nitrogen-doped reduced graphene oxide using fructose as precursor represented in Fig. 4. The mechanistic pathway suggested is based on the correlative
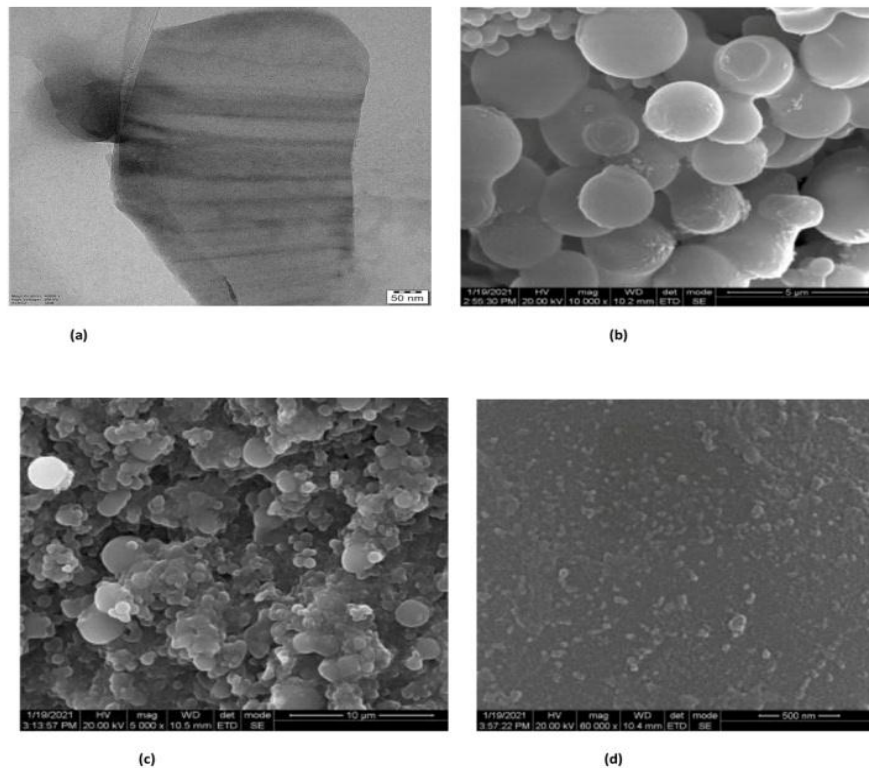

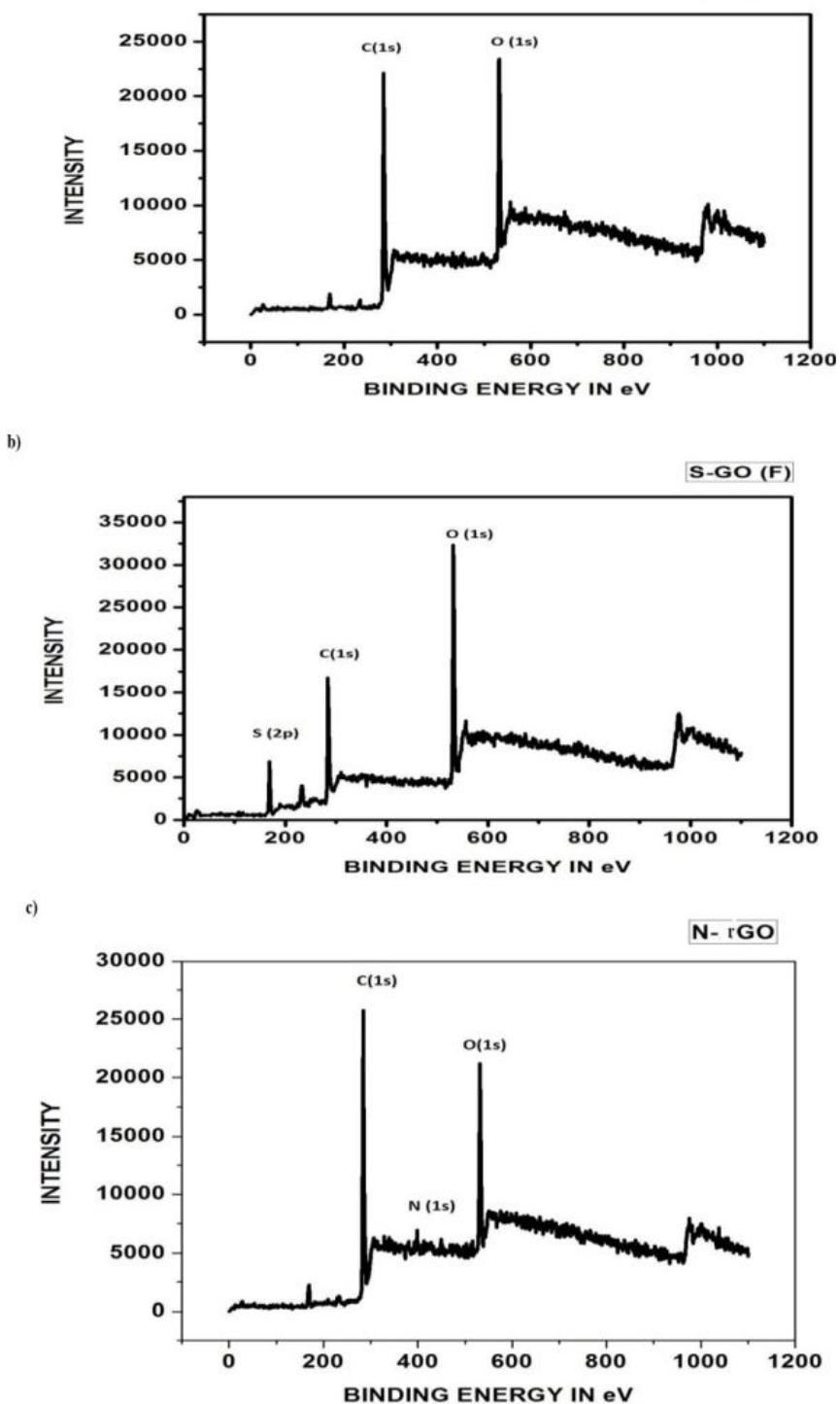Fig. 2: a). HR-TEM image of graphene oxide and FE-SEM images of b) CMs, c) S-GO, d). N-rGO.

Fig. 3: Wide scan X-ray photoelectron spectroscopy (XPS) images of a). Carbon microspheres b). Sulfur-doped graphene oxide and c). nitrogen-doped reduced graphene oxide.
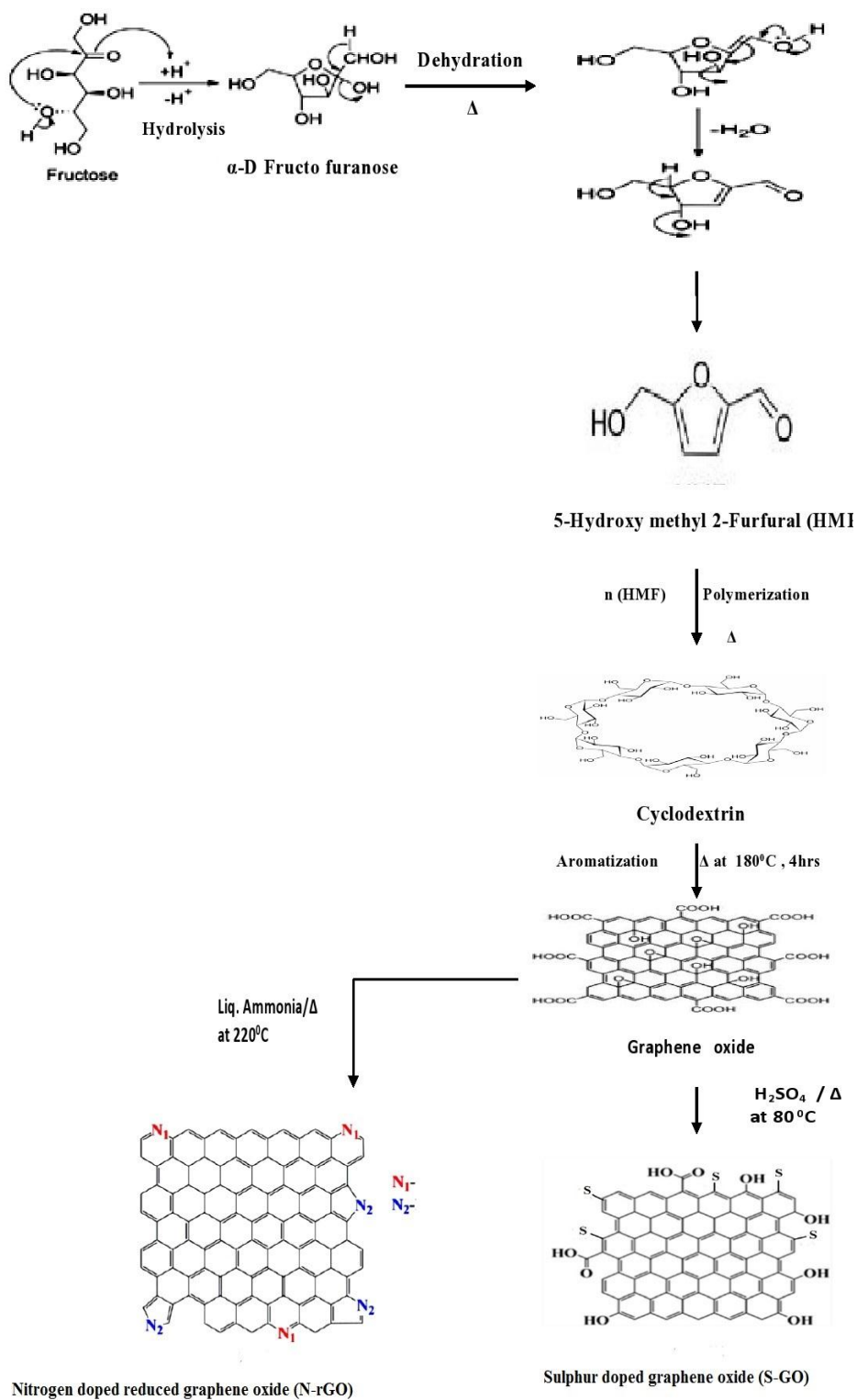
Fig. 4: A suggested reaction mechanism for the preparation of graphene oxide, sulfur-doped graphene oxide, and nitrogen-doped reduced graphene oxide from fructose as a precursor.

analytical results of the present study and not found in the literature.

Catalytic Application Study

Adsorption and photocatalytic decoloration of organic dyes (Methylene blue (MB), Methyl orange (MO), Rhodamine-Black (Rh. B) using as-synthesized samples as a catalyst: The experimental conditions were optimized for the decoloration of dyes using different (acidic, basic, and neutral) mediums under dark and UV light. The decoloration of dyes was found to be better under acidic conditions. Based on the optimization, the preliminary screening of the Catalytic decoloration of Methylene blue (MB), Methyl Orange (MO), Rhodamine-B (Rh-B) was carried out with the concentration of 2 ppm, $(2mg.10mL^{-1})$, pH=3 for 2 h in the dark, UV-light and Sunlight represented in Fig. 5.

The results indicate that all the sample shows adsorption property for the decoloration of organic dyes. Among the samples, the carbon microsphere has a good adsorbent feature due to the presence of uniform spherical-like morphology and the carboxyl functional group on the surface. Nurettin et al. (2017), reported that the maximum adsorption capacity of 67% for 0.1-g carbon microsphere for 50-ppm dye solu-

tions in DI water correlated with our report. The presence of oxygen-containing acidic functional groups in S-GO was effective in the photocatalytic activity for the removal of anionic dyes (methyl orange) and less acidic functional group on the surface in N-rGO was effective for the removal of cationic dyes (methylene blue and Rhodamine-B). This is due to the electronegative difference between the adsorbate and functional group existing on the surface of the adsorbent which enhanced surface defects in grain boundaries that are involved in the oxidation reaction for the decoloration of dyes under UV light and Sunlight.

From our results, S-GO was a more effective photocatalyst for the decoloration of dyes than N-rGO. The photocatalytic activity of S-GO was found to be more by using aldose as a precursor than ketose. It is attributed to the introduction of more heteroatoms, functional groups, elemental compositions existing on the surface with fewer structural defects as reported by Sudhaparimala et al. (2021).

Remediation of Toxic Heavy Metal Ions in Industrial Pollutants

Detection of copper and chromium ion using as-synthesized samples as adsorption catalyst by the colorimetric
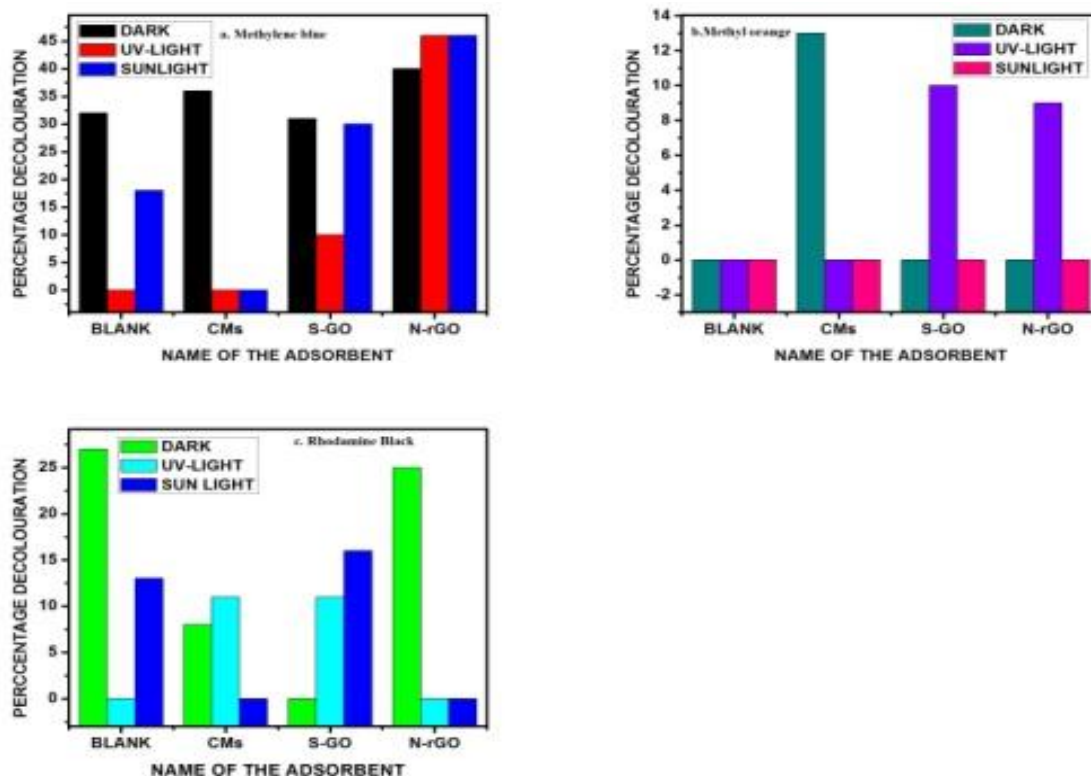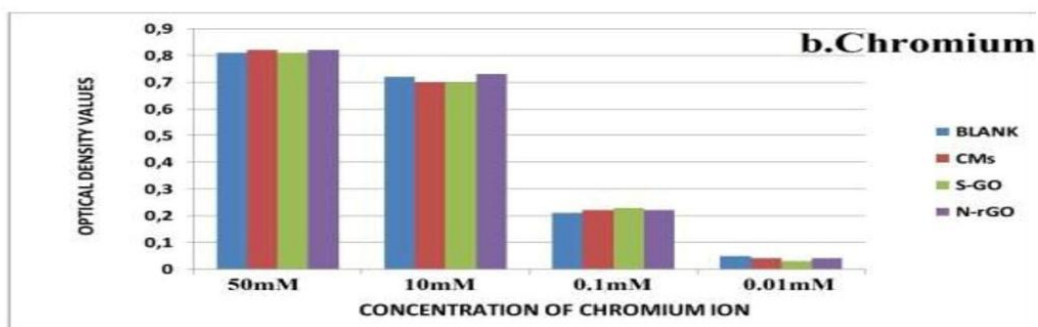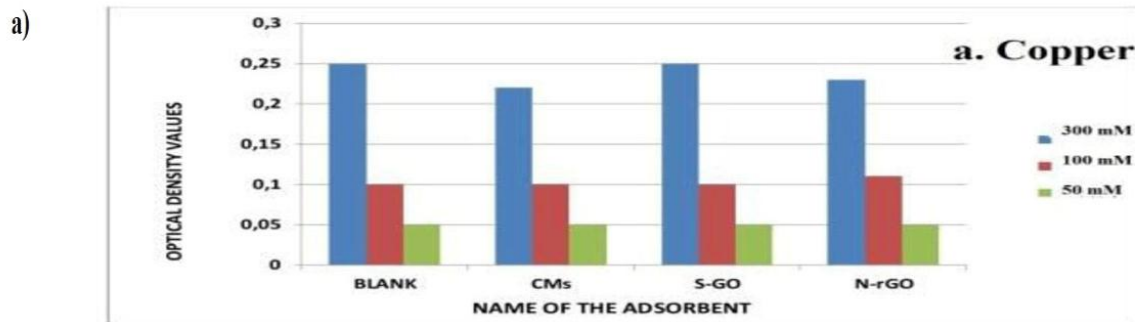

Fig. 5: Adsorption and photocatalytic decoloration of organic dyes a). Methylene blue (MB), b). Methyl orange (MO), c). Rhodamine-Black (Rh. B) using as-synthesized samples as a catalyst.
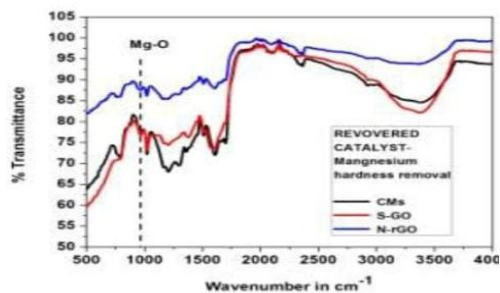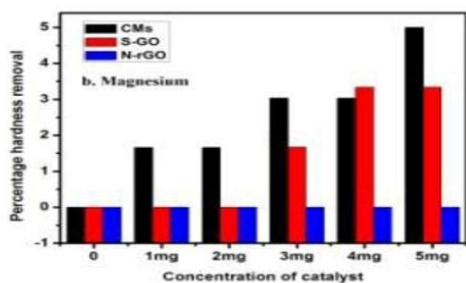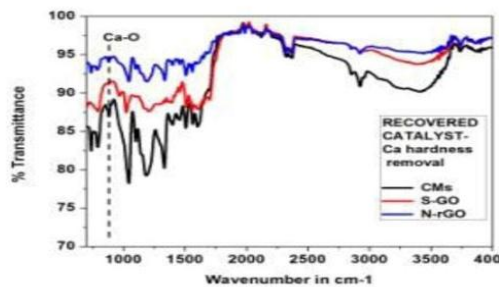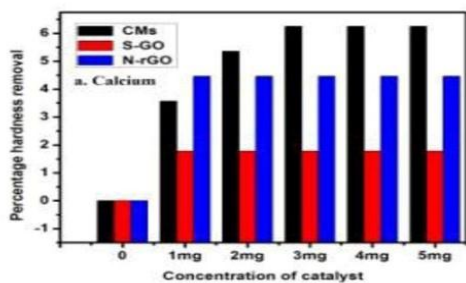
a)

b)

Fig. 6: 6(a) Detection of copper and chromium ion using as-synthesized samples as an adsorbent by colorimetric method, 6(b) estimation of a). Calcium ion b). Magnesium ion by using as-synthesized sample as an adsorbent by EDTA titration along with FTIR analysis of the recovered catalyst.

method: The preliminary screening of metal ions (Cu^{2+} and Cr^{6+}) detection was carried out individually using optical density values of different millimolar concentrations (300 mM, 100 mM, 50 mM) of copper sulfate and (50 mM, 10 mM, 0.1 mM, 0.01 mM) of metal ions and using a catalyst with the concentration of 100 ppm (w/v) and the results are represented in Fig. 6(a).

The effective adsorption of copper and chromium ions was detected at 300 mM and 0.01 mM concentrations respectively. The sample of CMs and N-rGO show a positive result for the detection of copper and chromium ion and S-GO shows a positive result for the detection of chromium ion. It may be due to the electronegativity difference between the adsorbate and adsorbent, morphology, and the functional groups existing on the surface as observed and correlated with SEM and XPS analysis. (Siti et al. 2020) reported that the interactions between graphene nanomaterial as adsorbents and heavy metals correlated with our report.

Estimation of calcium and magnesium ion in water using as-synthesized samples as adsorption catalyst by EDTA titration method

Limei et al. (2015) reported that EDTA functionalized magnetic graphene oxide (EDTA-mGO), a good adsorbent for Pb(II), Hg(II), and Cu(II). In this current study, the hardness of water (Ca^{2+} and Mg^{2+} ion) was detected by the EDTA titration method. In this study, the percentage hardness of water for the removal of heavy metal ions (Ca^{2+} and Mg^{2+}) was calculated by comparing with and without using a catalyst as represented in Fig. 6(b). All the synthesized samples showed activity in the removal hardness of Ca^{2+} or Mg^{2+} ion with increasing concentration of the catalyst. Among the three samples, the carbon microsphere showed better adsorption for (Ca^{2+} or Mg^{2+}) than S-GO and N-rGO due to the surface morphology and more carboxyl functional groups existing on the surface of CMs. The catalyst samples were recovered after the titration and the metal oxide stretching (Ca-O and Mg-O) was identified in the range of 900-1000cm^{-1} from FT-IR analysis

CONCLUSION

The study provided a simpler approach to the synthesis with the underlying principle in the conversion of ketose units to functionalized graphene structures and microspheres of carbon. The correlation of experimental parameters with the resulting structures provided the mechanistic pathway. The structure-activity relationship enabled the screening of their capacity to catalyze the degradation of amino dyes by adsorption and photocatalytic mode and exchange of heavy metal ions. The study of the influence of electronegativity of

the doped atoms (O, N and S), defects in the structure, and morphology upon their catalytic and ion exchange capacity adds more value. The results of the study will contribute much towards biomass conversion to smart nanomaterials, safe and efficient treatment of industrial (textile) wastewater. Finally, the study involving a simple precursor, lab set up, energy, and cost-saving approach provided important cues in the management of water pollution.

REFERENCES

Agata, Ś., Bartosz, G., Noel, D. and Grażyna, G. 2017. Nitrogen-doped reduced graphene oxide as electrode material for high rate supercapacitors. Appl. Surf. Sci., 399: 265-271.

Anton, S.M., Mikhail, A.V. and Peter, M.T. 2019. Solid-state 13C NMR of carbon nanostructures (milled graphite, graphene, carbon nanotubes, nanodiamonds, fullerenes) in 2000–2019: Fuller. Nanotubes Carbon Nanostr., 8: 1-14.

Bharatia, B., Sonkara, A.K., Singh, N., Dash, D. and Chandana, R. 2017. Enhanced photocatalytic degradation of dyes under sunlight using bio-compatible TiO2 nanoparticles. Mater. Res. Express, 4: 085503.

Erick, S., Lim, H., Nicole, K.A., Sara, P., Nahrizul, A.K., Ehsan, Z., Nasrul, A.B.A.R., Bahman, A.H. and Babak, S. 2020. Hydrothermal synthesis of carbon microspheres from sucrose with citric acid as a catalyst: Physico-chemical and structural properties. J. Taibah Univ. Sci., 14(1): 1042-1050.

Guangxu, H., Weiwei, K., Qianhao, G., Baolin, X., Quanrun, L., Jianbo, J. and Chuanxiang, Z. 2018. One-step green hydrothermal synthesis of few-layer graphene oxide from humic acid. Nanomaterials, 8(215): 1-9.

Hassan, A.F., Abdel-Mohsen, A.M. and Fouda, M.M.G. 2014. Comparative study of calcium alginate, activated carbon, and their composite beads on methylene blue adsorption. Carbohyd. Polym., 102: 192-198.

Ho, K., Maria, E., Fortunato, H.X., Jin, H.B. and Kenneth, S.S. 2011. Carbon microspheres as supercapacitors. J. Phys. Chem., 10: 1-6.

Isaac, C., Luis, J., Wonjun, P., Helin, C. and Yong, P.C. 2013. Raman spectroscopy of graphene and related materials. New Develop. Photon Mater. Res., 19: 1-20.

Limei, C., Yaoguang, W., Liang, G., Lihua, H., Liangguo, Y., Qin, W. and Bin, D. 2015. EDTA functionalized magnetic graphene oxide for removal of Pb(II), Hg(II), and Cu(II) in water treatment: Adsorption mechanism and separation property. Chem. Eng. J., 281: 1-10.

Mark, W., Joe, H. and Madison, W.I. 2011. The Raman spectroscopy of graphene and the determination of layer thickness. Thermo Fisher Sci., 6: 1-6.

Mingfei, P., Xiaoqian, X., Kaixin, L., Jingying, Y., Liping, Hong. and Shuo, Wang. 2020. Fluorescent carbon quantum dots-synthesis, functionalization, and sensing application in food analysis. Nanomaterials, 930(10): 1-25.

Mohammed, B.A. 2014. Removal of textile dyes (maxilon blue, and methyl orange) by date stones activated carbon. Int. J. Adv. Res. Chem. Sci., 1(1): 48-59.

Nurettin, S., Muhammad, F., Saif, U.R., Selin, S.M., Sahiner, M.S. and Nahit, A. 2017. Synthesis, characterization, and use of carbon microspheres for removal of different dyes from aqueous environments. Water Air Soil Pollut., 228(10): 1-10.

Qinghong, W., Can, G., Yuxuan, Z., Jiapeng, H. and Hongqiang, W. 2018. Reduced graphene oxide-wrapped fes2 composite as anode for high-performance sodium-ion batteries. Nanomicro Lett., 10(30): 1-9.

Rao, C.N.R., Venkataraghvan, R. and Kasturi, T.R. 1963. Contribution of the infrared spectra of organao sulfur compound. Canad. J. Chem., 6: 636-42.

Sanja, K., Branka, K., Vladimir, D., Andjelka, Z. and Bjelajac, R. 2015. Structural properties of carbon microspheres obtained by hydrothermal treatment of fructose. Sci. Paper, 56: 155-158.

Shunjian, X., Yufeng, L., Wei, Z., Zonghu, X., Yongping, L., Hui, O., Huanwen, W. and Feng, Y. 2015. Synthesis of carbon microspheres from saccharides based on the hydrothermal process. Int. Conf. Mater. Chem. Environ. Protect., 5: 1-15.

Siti, Z.N.A., Wan, N.S., Ahmed, F.S., Norhariza, Y., Mohd, Z.M., Mohd, Y. and Farhana, A. 2020.Adsorptive removal of heavy metal ions using graphene-based nanomaterials: Toxicity, roles of functional groups and mechanisms. Chemosphere, 248: 1-15.

Sudhaparimala, S. and Usha, R. 2021. Functionalization of graphene with O and S for catalytic degradation of chlorophenols and dyes. Mater. Sci. Forum, 1019: 194-204.

Sudhaparimala,S. and Usha, R. 2020. Energy-efficient functionalization of graphene for tunable fluorescence. IOP Sci. – J. Phys. Conf. Ser., 1706: 1-12.

Sunil, K.C., Saritha, S., Rajesh, K.N., Chethan, G., Mustak, M.S. and Narayana, Y. 2020. Facile, cost-effective, and eco-friendly synthesis of carbonyl-rich partially reduced graphene oxide using glucose as a sole precursor. SN Appl. Sci., 2(1323): 1-8.

Tapas, K.D., Seemita, B., Pandey, M., Vishwanath, B., Kshirsagar, R.J. and Sudarsan, V. 2016. Effect of surface functional groups on hydrogen adsorption properties of Pd dispersed reduced graphene oxide. Int. J. hydro.Energy, 6: 1-10.

Van Ael, E. Covaci, A., Blust, R. and Bervoets, L. 2012. Persistent organic pollutants in the Scheldt estuary: Environmental distribution and bio-accumulation. Environ. Int., 48: 17-27.

Vasilios, G., Jason, A., Perman, M., Jiri, T. and Radek, Z. 2015. A broad family of carbon nanoallotropes: Classification, chemistry and applications of fullerenes, carbon dots, nanotubes, graphene, nanodiamonds, and combined superstructures. Chem. Rev., 115: 4744-4822.

Zhangting, W. and Zhenhua, N. 2017. Spectroscopic investigation of defects in two-dimensional materials. Nanophotonics, 6(6): 1219-1237.